

Supplemental Figures:

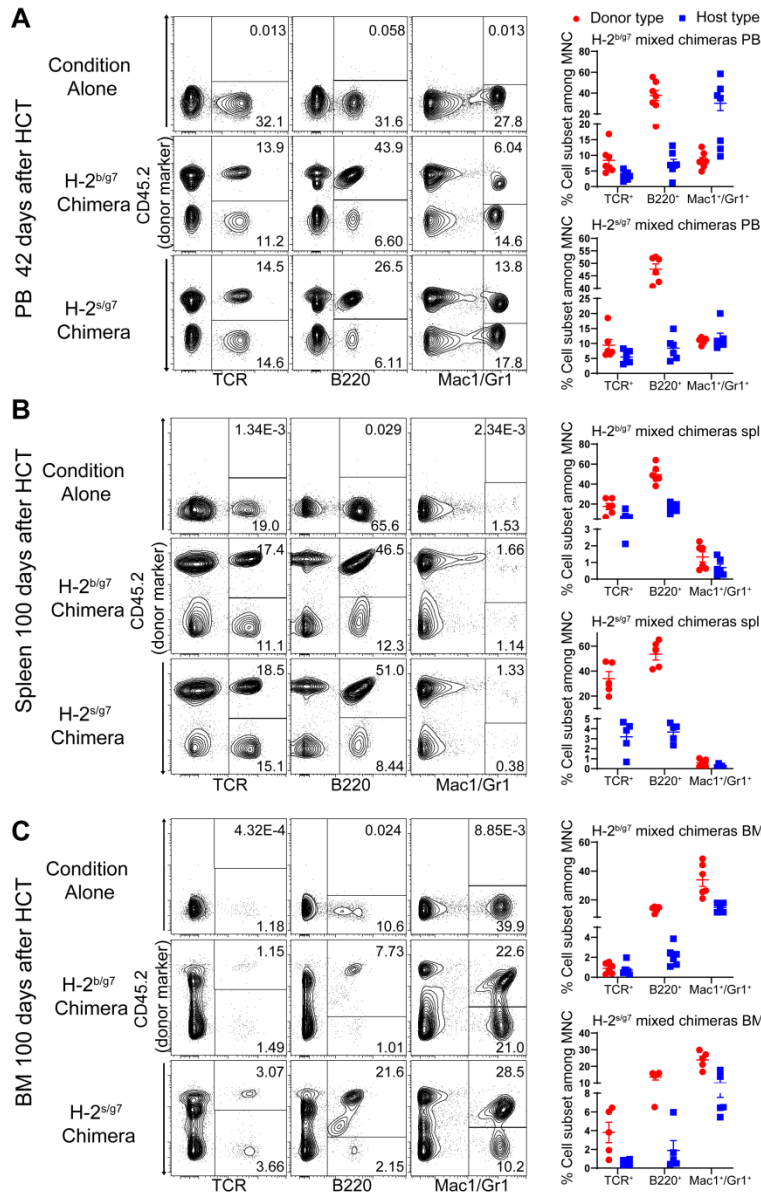


Fig. S1: Haplo-MC status is achieved in WT NOD mice with haploidentical donors. Prediabetic 9-12 weeks old NOD mice were conditioned with ATG + CY + PT, and transplanted with BM (50×10^6) and SPL cells (30×10^6) from H-2^{b/g7} F1 or H-2^{s/g7} F1 donors respectively, and co-injected with depleting anti-CD4 mAb (500 μ g/mouse). The recipients were monitored for chimerism in the peripheral blood and levels of blood glucose. **(A)** A representative flow cytometry pattern of T cells (TCR β^+), B cells (B220 $^+$), and myeloid cells (Mac1/Gr1 $^+$) in the peripheral blood at 6 weeks after HCT and mean \pm SE of percentage of donor- and host-type cells of 5-7 representative mice for 12 mice in each group combined from two replicate experiments. **(B and C)** Spleen and bone marrow samples from chimeric WT NOD or conditioning alone control were collected at day100 for validating the chimerism status. One representative flow cytometry pattern and Mean \pm SE of percentage of 5 representative mice in each group are shown for total 12 mice from two replicate experiments.

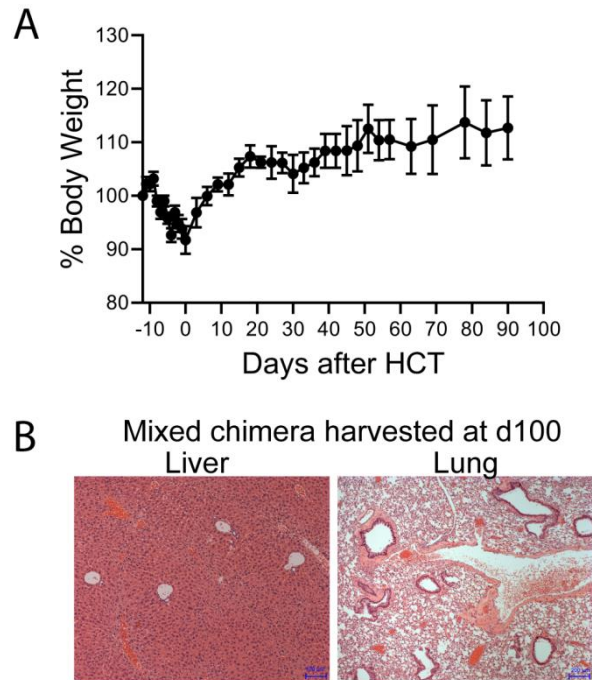


Fig. S2: No sign of clinical or tissue GVHD is observed in Hapo-MC WT NOD mice.

Bodyweight of WT NOD mice in Figure 1 was monitored for 100 days after HCT. At d100, Liver and lung samples were collected and subjected to HE staining to evaluate GVHD histopathology. **(A)** Body weight curve of 12 mice is shown. **(B)** One representative liver and lung tissue microphoto is shown of 5 mice examined in each group.

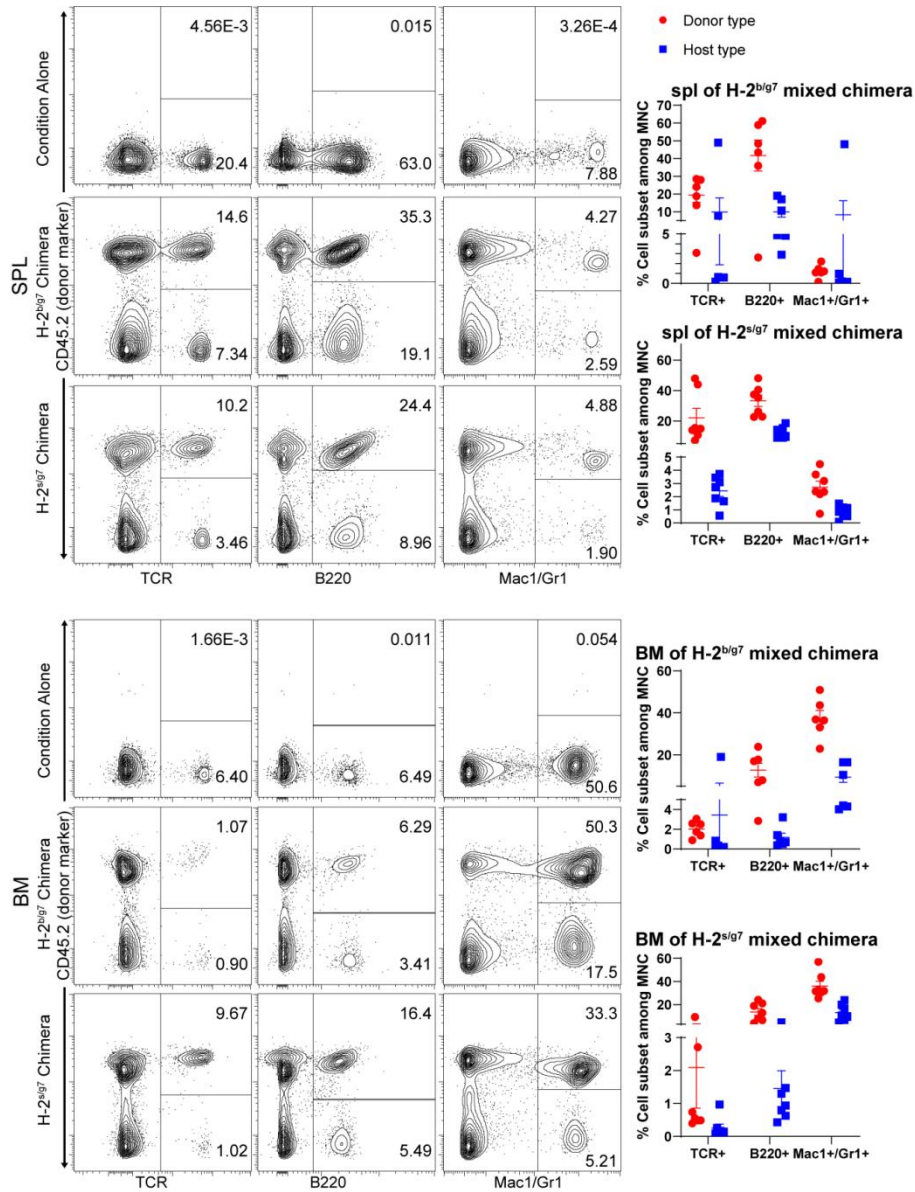


Fig. S3: Haplo-MC status is achieved in BDC2.5 NOD mice with haploidentical donors. 6-9 weeks old BDC2.5 NOD mice were conditioned with ATG + CY + PT, and transplanted with BM (50×10^6) and SPL cells (30×10^6) from H-2^{b/g7} F1 or H-2^{s/g7} F1 donors, respectively, co-injected with depleting anti-CD4 mAb (500 μ g/mouse). The recipients were monitored for mixed chimerism in the peripheral blood and glucose levels of blood. Haplo-MC status of T, B, and myeloid cells was validated with spleen and bone marrow MNC at the end of experiments at 60 days after HCT. One representative flow cytometry pattern and Mean \pm SE of percentage of 5-7 representative mice in each group are shown for 10 mice from two replicate experiments. The T1D development curve is shown in Fig. S19.

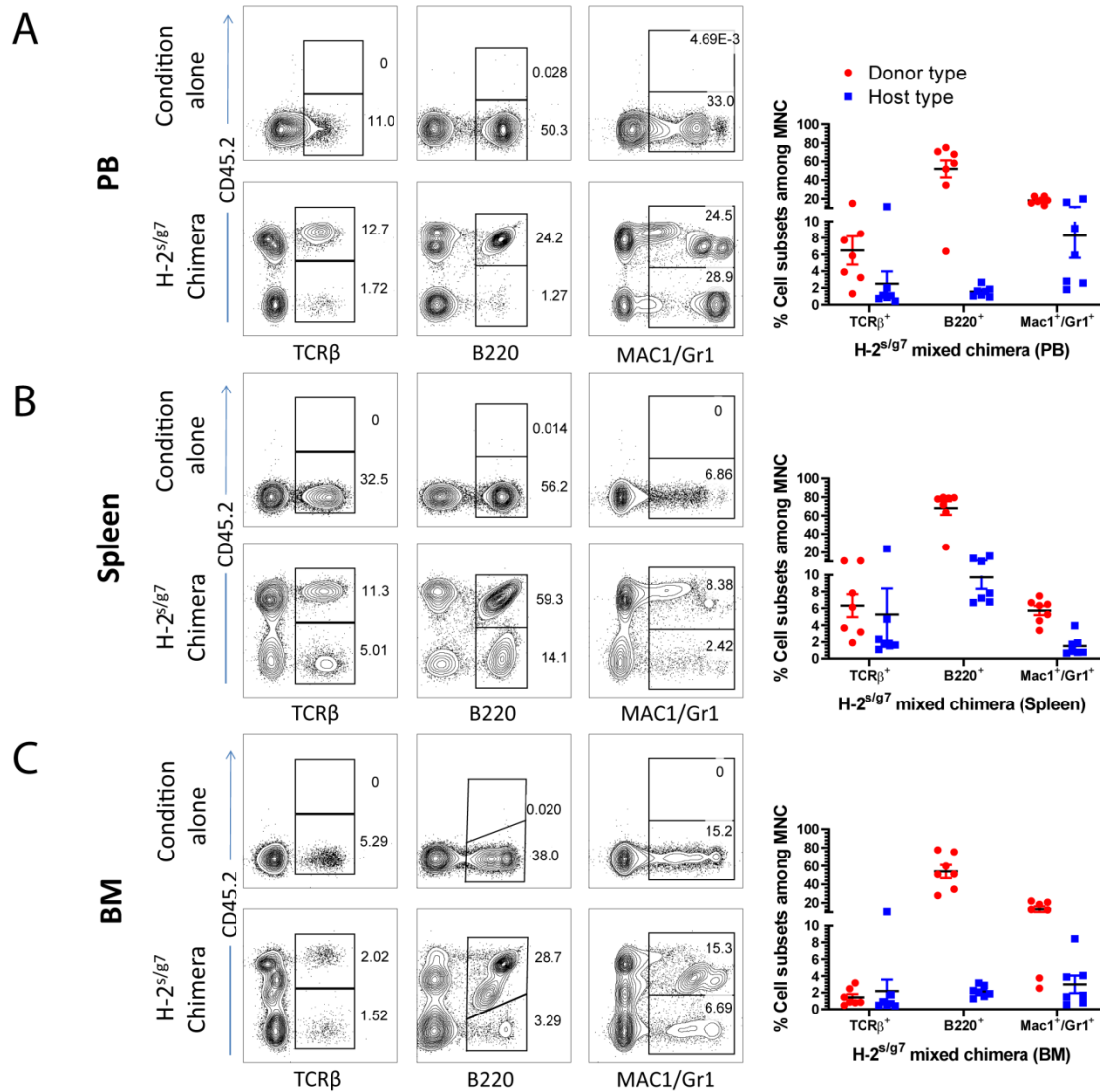


Fig. S4: Haplo-MC is achieved in thymectomized WT NOD mice. WT-NOD mice were given thymectomy at age of 6-week by JAX lab. 3-4 weeks after thymectomy, mice were conditioned with ATG + CY + PT and transplanted with BM (50×10^6) from H-2^{s/g7} F1 donors. Recipients were monitored for chimerism in the blood and levels of blood glucose for up to 80 days after HCT. At the end of experiments, recipients were validated for mixed chimerism status of T cells (TCRβ⁺), B cells (B220⁺), and myeloid cells (Mac1/Gr1⁺) in the peripheral blood (A), spleen (B) and BM (C). One representative flow cytometry pattern and mean \pm SE of percentage of 5-7 representative mice are shown for totally 10 mice in two replicate experiments.

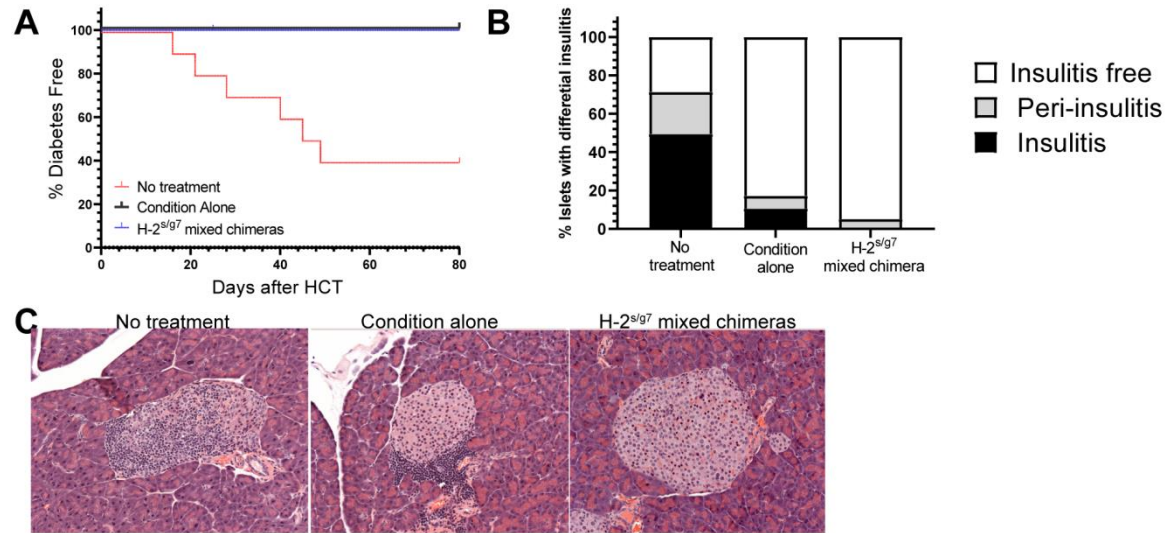


Fig. S5: Haplo-MC prevents T1D development and eliminate insulinitis in thymectomized WT NOD mice. The same thymectomized NOD mice with Hapo-MC described in **Fig. S4** were monitored for T1D development and evaluated for insulinitis at the end of experiments. **(A)** T1D development curves, 10 mice/group combined from two replicate experiments. **(B-C)** Insulinitis score and representative insulinitis microphotographs of mice that did not show hyperglycemia by the end of experiments are shown for 4-6 mice examined in each group.

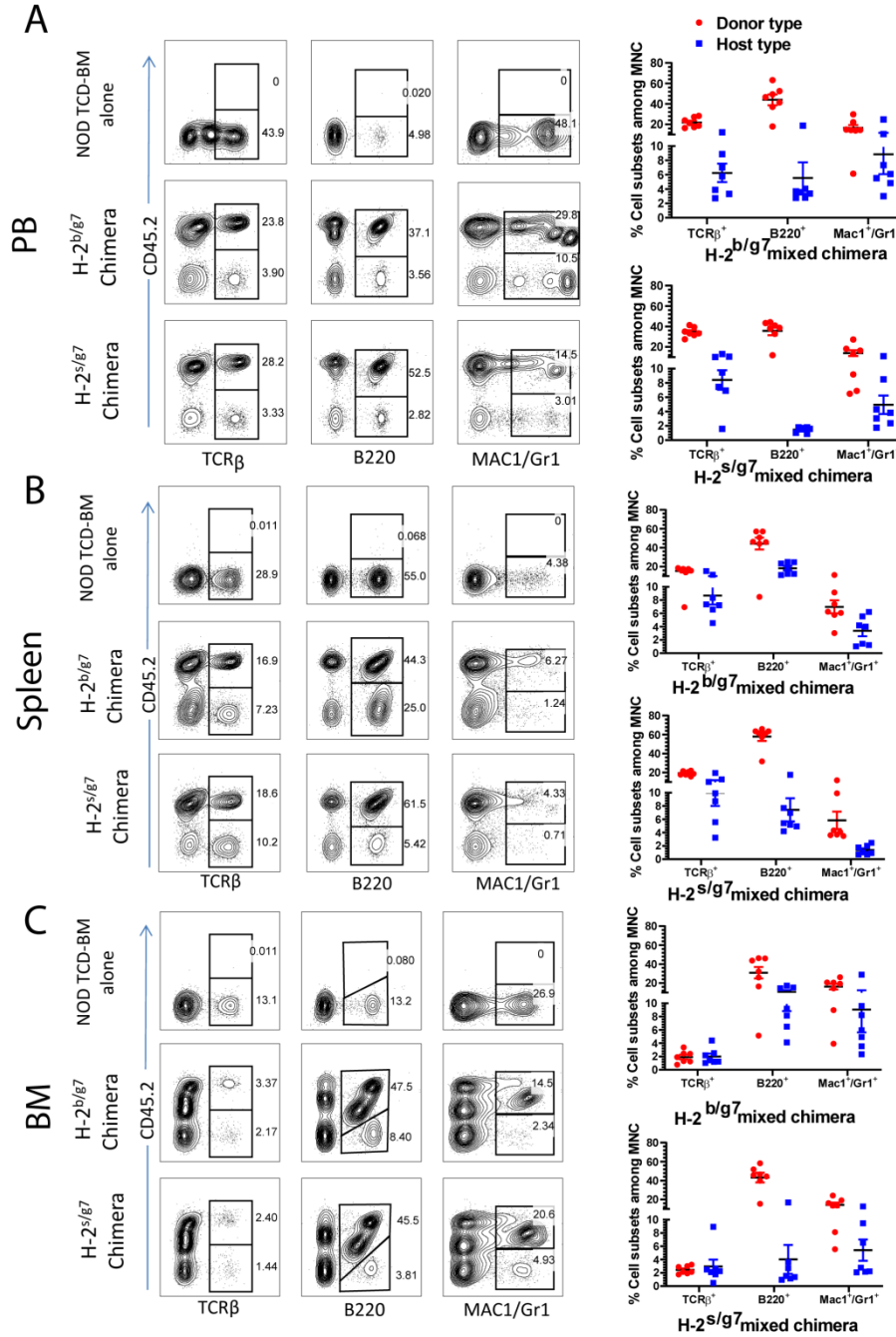


Fig. S6: Haplo-MC status is achieved in lethal TBI-conditioned WT NOD mice. Prediabetic 9-12 weeks old NOD mice were conditioned with lethal TBI (950cGy) and transplanted with syngeneic TCD-BM (5×10^6) from NOD mice and haplo-TCD-BM (7.5×10^6) from H-2^{b/g7} or H-2^{s/g7} F1 donors. Control recipients were transplanted with TCD-BM from NOD mice only. Recipients were monitored for chimerism in the peripheral blood and levels of blood glucose for 80 days after HCT. At the end of experiments, recipients were validated for chimerism status of T cells (TCR β ⁺), B cells (B220⁺), and myeloid cells (Mac1/Gr1⁺) in the peripheral blood (A), spleen (B) and BM (C). One representative flow cytometry pattern and Mean \pm SE of percentage of 7 representative mice are shown for total 10-15 mice from two replicate experiments.

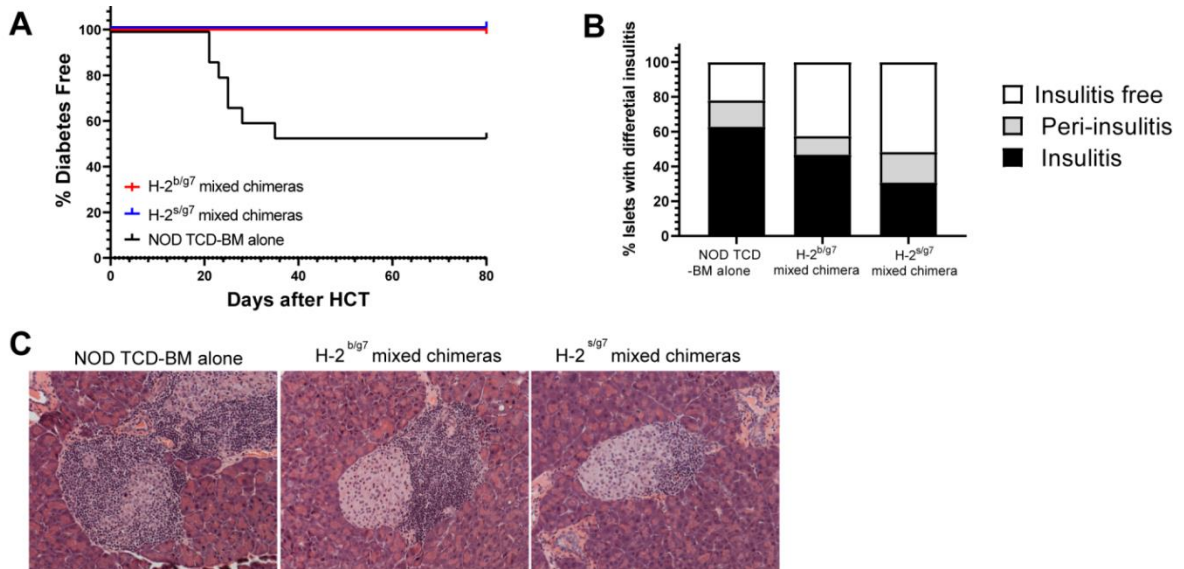


Fig S7: Induction of Haplo-MC in lethal TBI-conditioned mice does not eliminate insulinitis although prevents clinical T1D. Lethal TBI-conditioned WT NOD mice were induced to developed Haplo-MC and monitored for T1D development as described in Fig. S6. Recipients were monitored for diabetes development for 80 days after HCT. **(A)** T1D development curves in prediabetic NOD mice. There were 10-15 mice combined from two replicate experiments. **(B-C)** 80 days after HCT, residual non-diabetic mice were subject to insulinitis evaluation. Summary insulinitis score and representative islet microphotographs (magnification 10 \times) are shown for 5-10 representative mice from two replicate experiments.

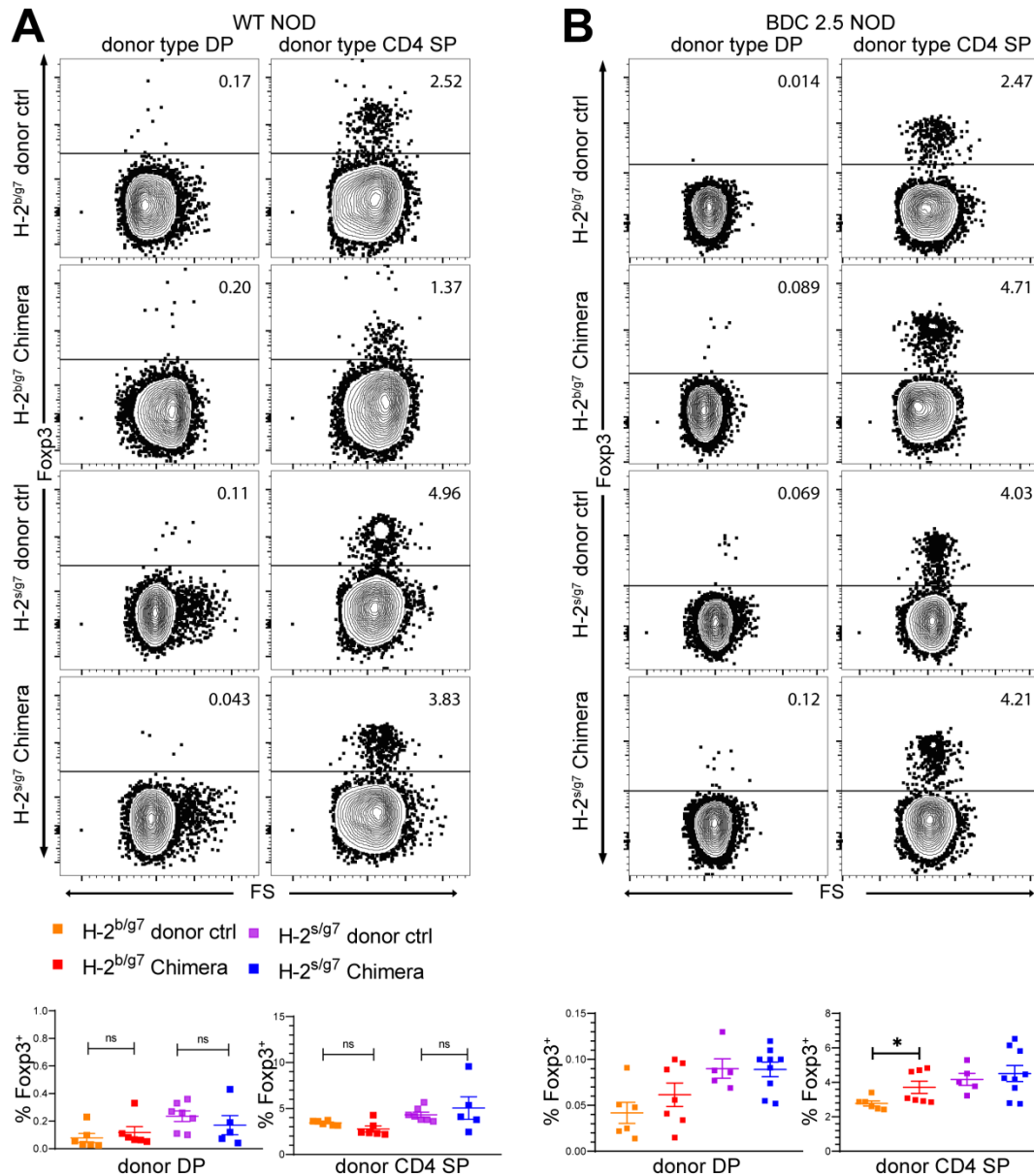


Fig S8: Increase of donor-type tReg production in thymus is observed in transgenic BDC2.5 but not in WT NOD Haplo-MC. 60 days after HCT, H-2^{b/g7} and H-2^{s/g7} Haplo-MC mice of WT NOD (**A**) and BDC2.5 NOD (**B**) and control donor mice were measured for donor-type Fcγp3⁺ Treg cells among CD4⁺CD8⁻ (CD4 SP) cells or CD4⁺CD8⁺ (DP) cells in the thymus. Representative flow cytometry patterns and mean ± SEM of tReg percentage among donor-type SP or DP thymocytes are shown for 5-7 mice for in each group from two replicate experiments. *p<0.05.

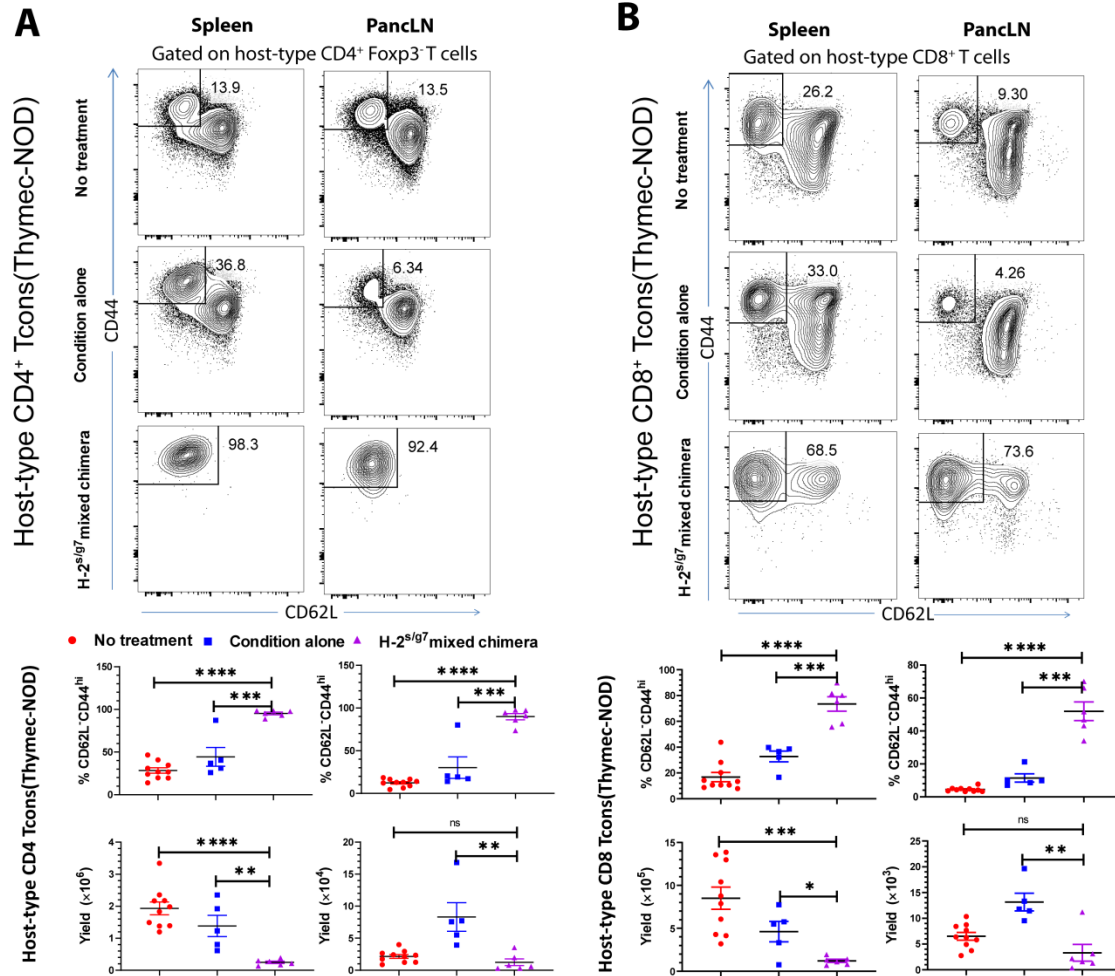


Fig S9: Haplo-MC reduces host-type T effector memory cells in thymectomized WT NOD mice. Thymectomized NOD mice with or without induction of Haplo-MC described in Fig S4 were further analyzed for residual host-type T cell subset at the end of experiments. Mononuclear cells (MNC) of spleen and pancreatic LN of mice with Haplo-MC, mice given conditioning only and mice given no treatment were analyzed by flow cytometry for percentage of host-type CD44^{hi}CD62L⁻ CD4⁺ T (A) or CD8⁺ T (B) T effector memory cells. A representative flow cytometry pattern and mean \pm SE of percentage and yield of CD44^{hi}CD62L⁻ effector memory T cells are shown of 5-10 representative mice in each group from two replicate experiments. * $p < 0.05$, ** $p < 0.01$, *** $p < 0.001$, **** $p < 0.0001$.

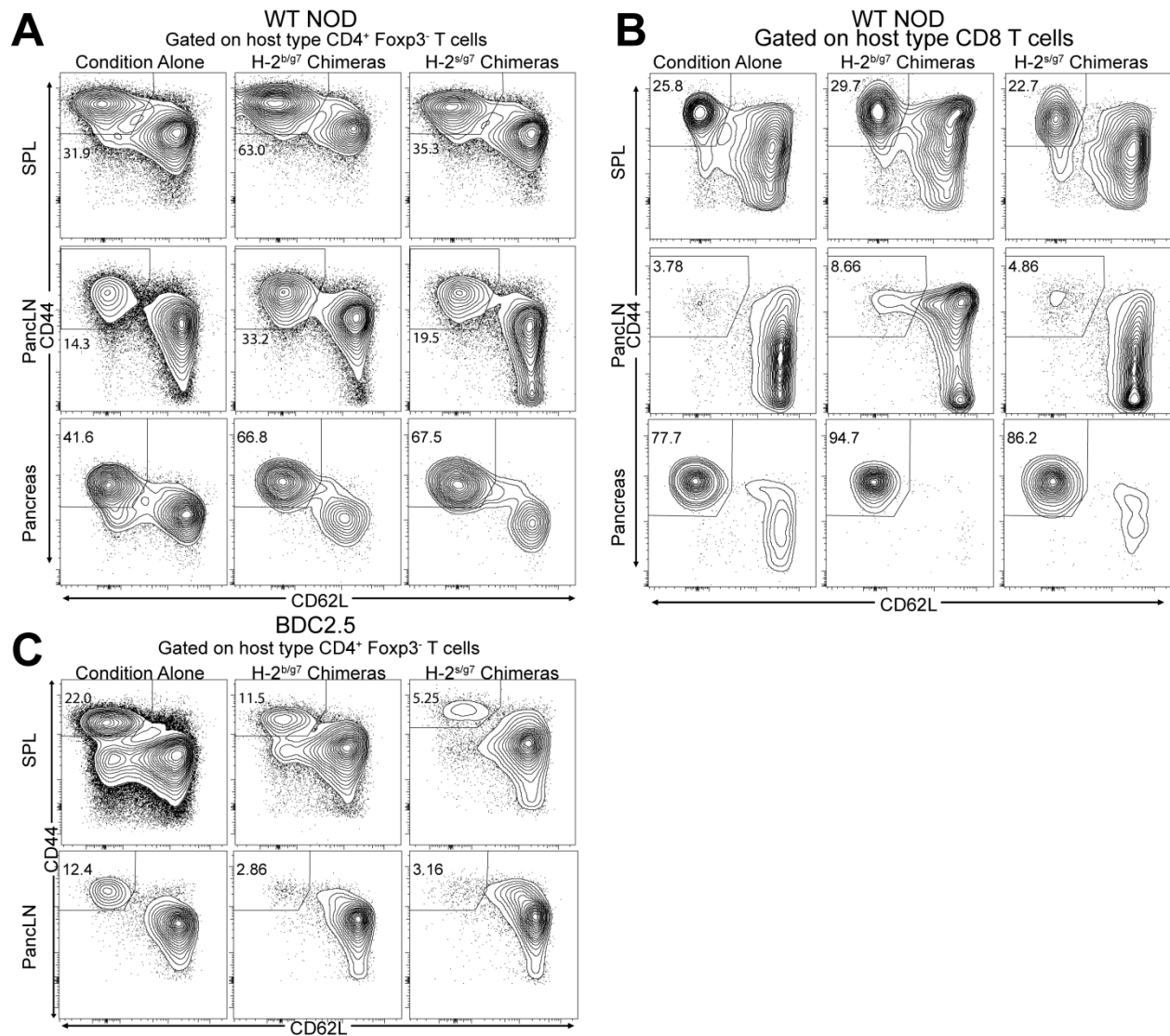


Fig S10: A supplement of representative flow cytometry patterns for Fig. 4: Haplo-MC reduces host-type autoreactive CD4⁺ and CD8⁺ T effector cells in WT and BDC2.5 NOD mice. 60 days after HCT, MNC of SPL, PancLN and pancreas from WT and BDC2.5 mixed chimeras and control mice were analyzed with flow cytometry for percentage of CD45.1⁺ host-type T effector cells (CD45.1⁺CD44^{hi}CD62L⁻TCRβ⁺). One representative pattern is shown for **(A)** host type CD4⁺ Tcon in WT NOD mixed chimeras, **(B)** CD8⁺ T cells in WT NOD mixed chimeras and **(C)** host-type CD4⁺ Tcon in BDC 2.5NOD mixed chimeras.

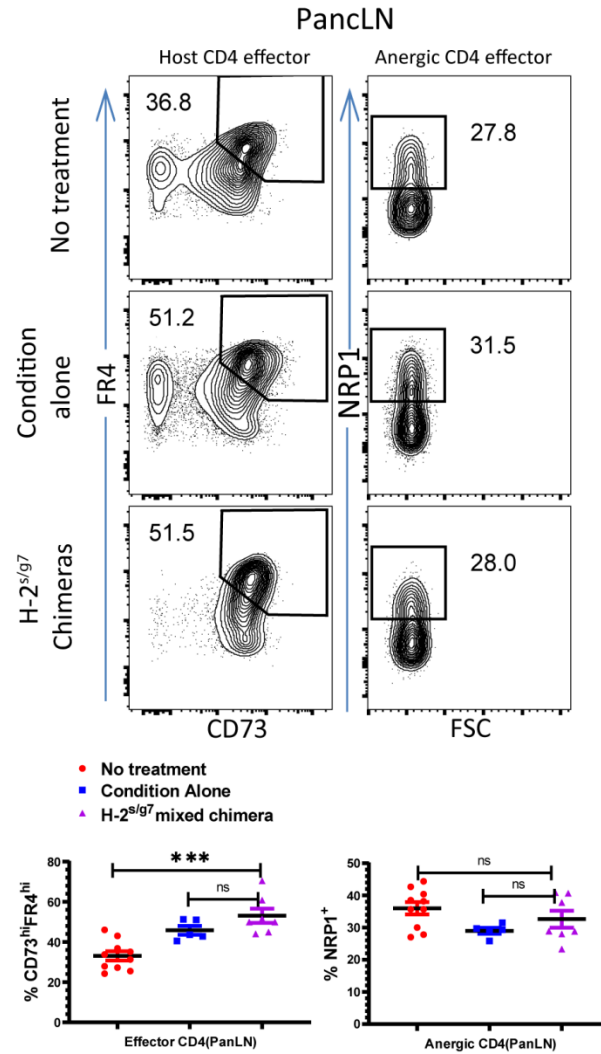


Fig. S11: Haplo-MC in thymectomized NOD mice does not increase Nrp-1⁺ cells among host-type residual CD73⁺FR4⁺ anergic CD4⁺ Tem cells. Thymectomized NOD mice with or without induction of Haplo-MC described in Fig S4 were further analyzed for anergy status of residual host-type T cells. MNC from PanLN of mice with Haplo-MC, mice given conditioning only, and mice given no treatment were analyzed by flow cytometry for their expression of CD45.1(host-marker), TCR β , CD4, Foxp3, CD62L, CD44, CD73, FR4 and Nrp-1. Representative patterns of flow cytometry and mean \pm SEM of percentage of anergic CD73^{hi}FR4^{hi} cells among CD4⁺Foxp3⁻CD62L⁻CD44^{hi} Tem cells and percentage of Nrp-1⁺ cells among anergic CD73^{hi}FR4^{hi} Tem cells are shown for 5-10 mice in each group. ***p<0.001.

Gated on host type Foxp3⁺ CD4⁺ cells

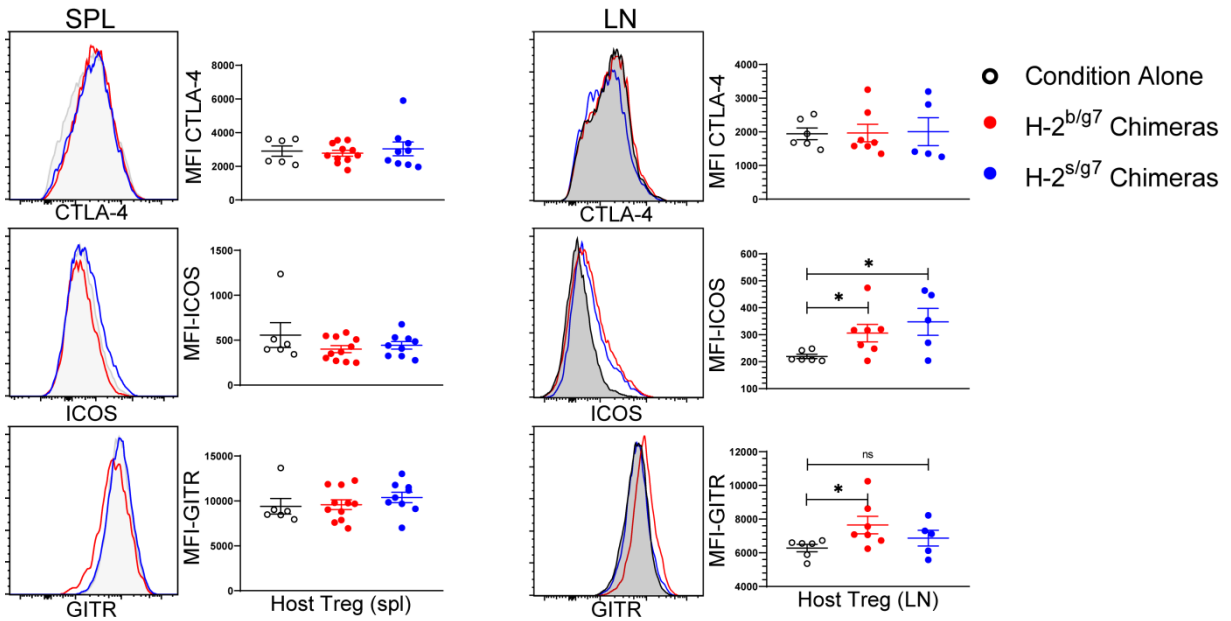


Fig S12: Host-type Tregs in euthymic NOD mice with Haplo-MC upregulate expression of activation markers. 60 days after HCT, host-type CD45.1⁺Foxp3⁺CD4⁺ Treg cells in the spleen and pancreatic LN were analyzed for surface markers of CTLA4, ICOS and GITR. Representative patterns and Mean \pm SEM of medium fluorescent intensity (MFI) of CTLA-4, ICOS and GITR expressed on host-type tTreg cells are shown for 5-11 mice in each group. *p<0.05.

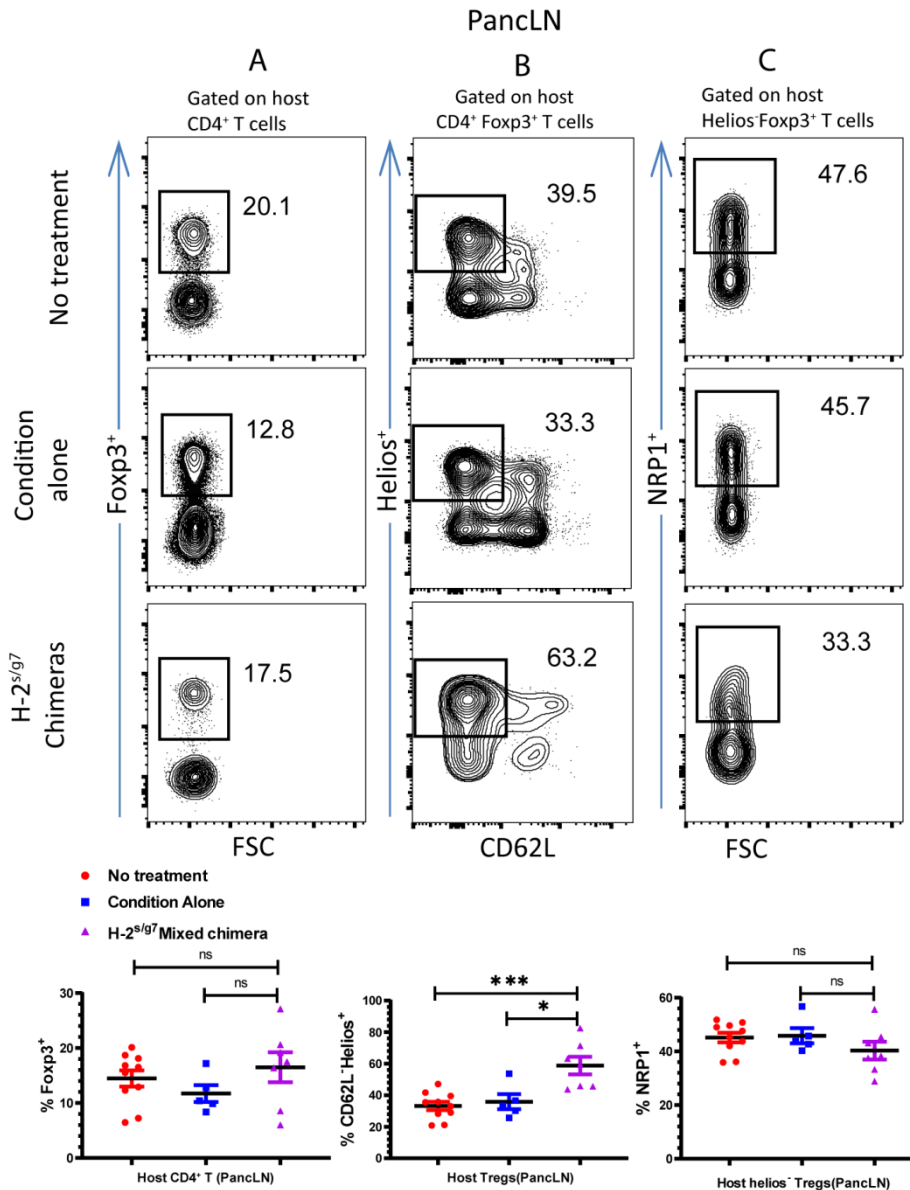


Fig S13: Haplo-MC in thymectomized NOD mice increases host-type CD62L⁺Helios⁺ tTreg but not CD62L⁻Helios⁻Nrp-1⁺ pTreg cells. Thymectomized NOD mice with or without induction of Haplo-MC described in Fig S4 were further analyzed for host-type Treg subsets among residual host-type T cells from PancLN of mice with Haplo-MC, mice given conditioning alone and mice without treatment. **(A)** gated Foxp3⁺CD4⁺ Treg cell are shown in Foxp3 versus FSC; **(B)** gated Foxp⁺CD4⁺ Treg cells are shown in Helios versus CD62L; **(C)** gated Helios⁻ Treg cells are shown in Nrp-1 versus FSC. Mean ± SE of percentage of Foxp3⁺CD4⁺ Treg cells among total host-type CD4⁺ T cells, Helios⁺ tTreg cells among total Treg cells, and Nrp-1⁺ pTreg cells among Helios⁻ Treg cells are shown below columns **A**, **B** and **C**, respectively. There are 5-10 mice in each group. *p<0.05, ***p<0.001.

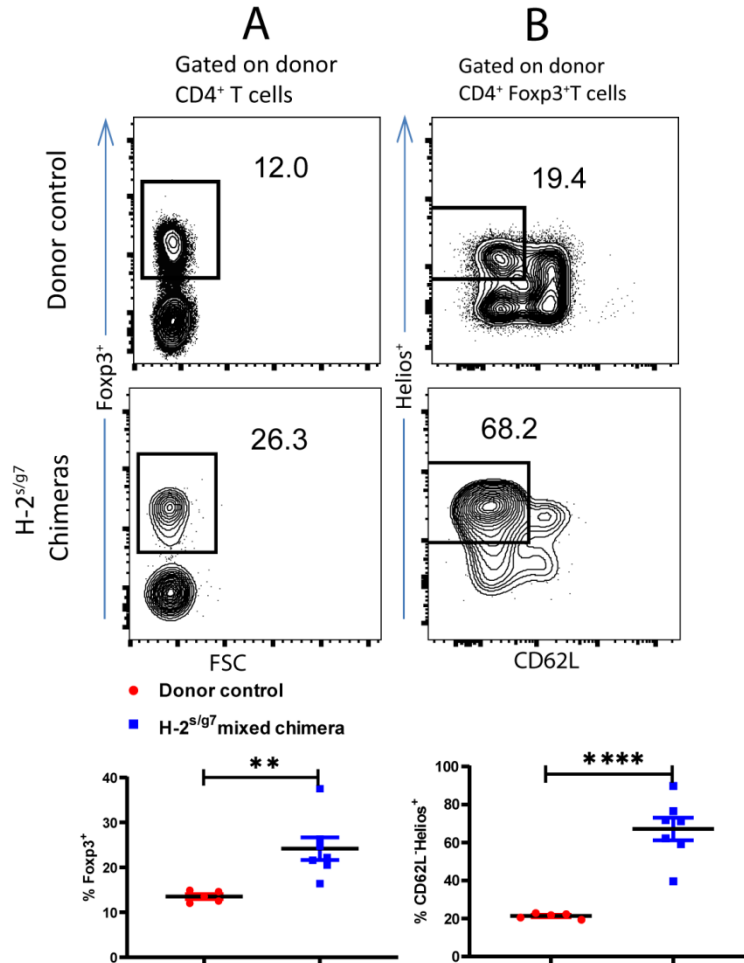


Fig S14: Haplo-MC in thymectomized NOD mice increases donor-type CD62L⁻ Helios⁺ tTreg cells. Thymectomized NOD mice with Haplo-MC described in Fig S4 were compared with donor mice for tTreg subsets in the PancLN. **(A)** gated Foxp3⁺CD4⁺ Treg cells are shown in Foxp3 versus FSC; **(B)** gated Foxp⁺CD4⁺ Treg cells are shown in Helios versus CD62L. Mean \pm SE of percentage of Foxp3⁺CD4⁺ Treg cells among total host-type CD4⁺ T cells, Helios⁺ tTreg cells among total Treg cells are shown below columns **A** and **B**, respectively. There are 5-10 mice in each group. **p<0.01, ****p<0.0001.

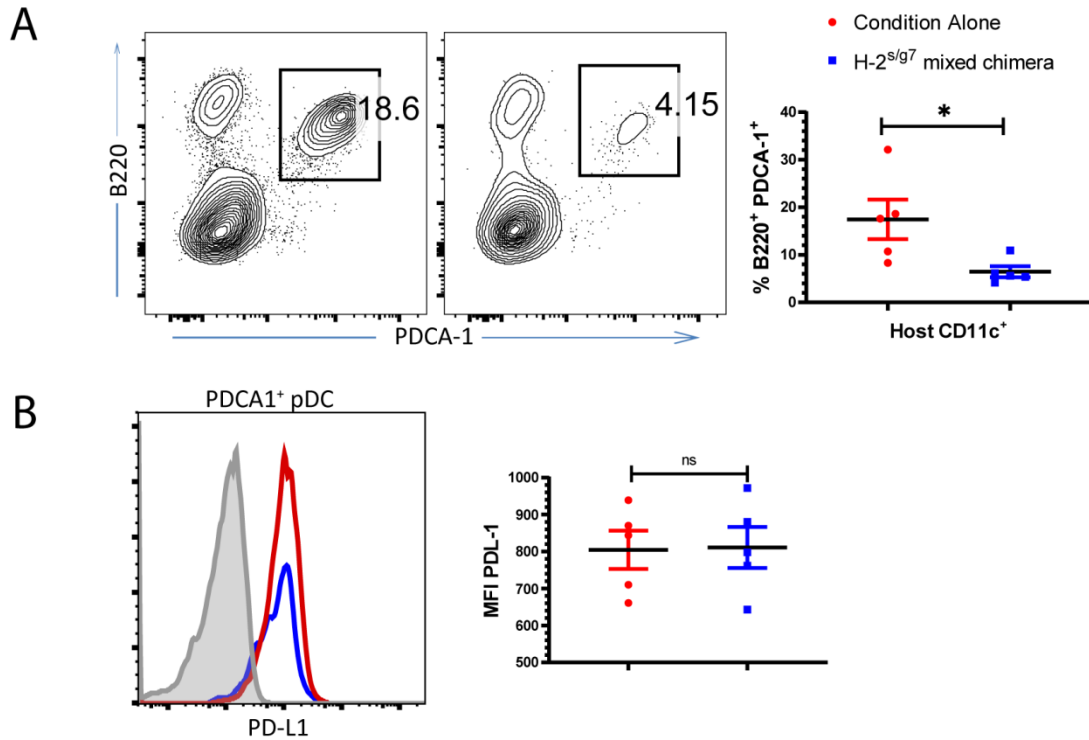


Fig S15: Haplo-MC in thymectomized NOD mice reduces host-type pDC without changing their PD-L1 expression. Thymectomized NOD mice with Haplo-MC described in Fig S4 were further analyzed for DC subsets. MNC from spleen of mice with Haplo-MC and mice given conditioning alone were analyzed for percentage of host-type IgM⁻IgD⁻CD11c⁺B220⁺PDCA1⁺ pDCs and their expression of PD-L1. **(A)** Representative pattern and mean \pm SEM of percentage of host-type B220⁺PDCA-1⁺ pDC (n=5-7). **(B)** Representative patterns and mean \pm SEM of PD-L1 expression levels on host-type pDCs population in comparison to control mice. N=5-7. *p<0.05.

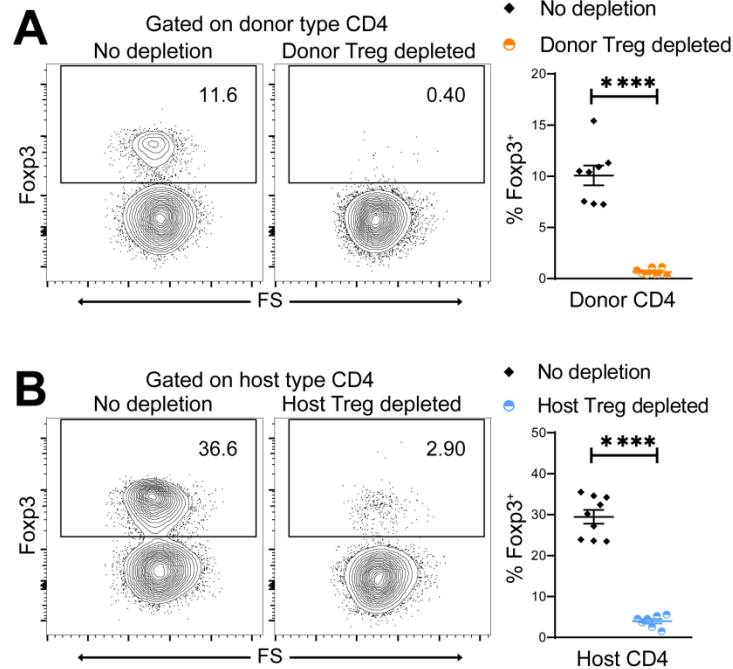


Fig S16: Effective depletion of donor- or host-type Treg cells occurred after DT injections. Mixed chimerism was induced using either donor or host mice carrying Foxp3^{DTR}. 45-60 days after HCT, diphtheria toxin (DT) was injected to chimeric mice every 3 days for 21 days. Only Foxp3⁺ Treg cells from Foxp3^{DTR} carrying mice can express DT receptor and would be depleted. **(A)** Depletion of donor-type Treg cells among MNC of SPL cells of mixed chimeras with donor cells carrying Foxp3^{DTR}. Representative pattern and Mean \pm SEM of percentage of Foxp3⁺CD4⁺ T cells among donor-type CD4⁺ T cells are shown, n=7-8. **(B)** Depletion of host-type Treg cells among MNC of SPL cells of mixed chimeras with host cells carrying Foxp3^{DTR}. Representative pattern and Mean \pm SEM of percentage of Foxp3⁺CD4⁺ T cells among host-type CD4⁺ T cells are shown. n=7-9. ****p<0.0001.

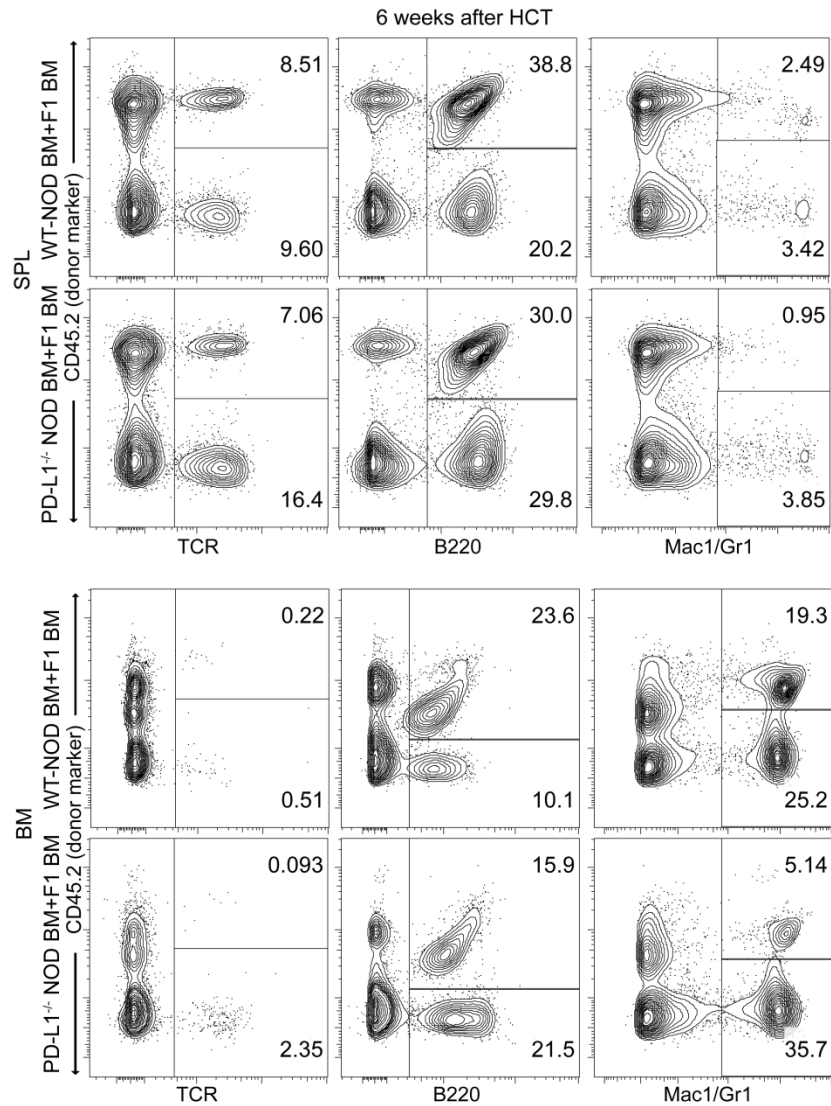


Fig S17: Mixed chimerism status is achieved in WT NOD mice by co-transplanting TCD-BM from H-2^{b/g7} F1 donor and WT or PD-L1^{-/-} host NOD mice. TCD-BM from H-2^{b/g7} F1 was mixed with TCD-BM from either WT or PD-L1^{-/-} NOD mice and injected into lethally irradiated WT NOD recipients. Recipients were monitored for chimerism in blood and levels of blood glucose. Six weeks after HCT, 5 mice from each group were used for validation of Haplo-MC by analyzing mixed chimerism status of T, B and macrophage/granulocytes in the spleen and BM. Representative staining patterns are shown.

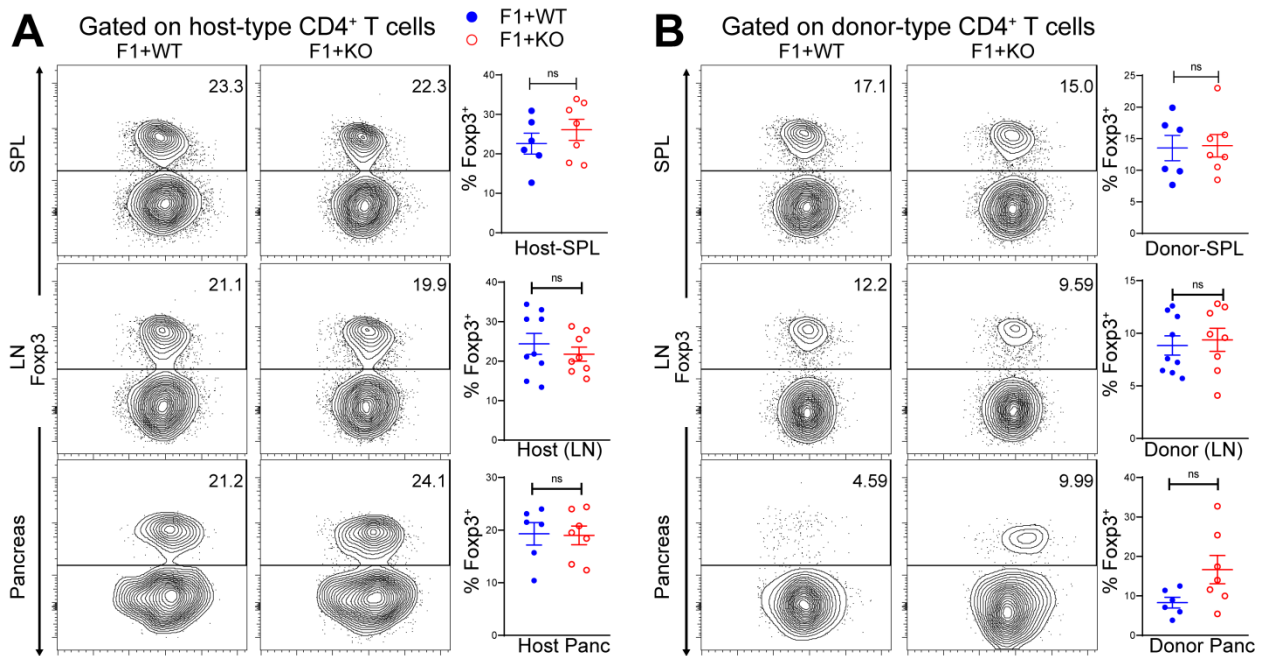


Fig S18: PD-L1 deficiency in host-type hematopoietic cells causes no changes in the donor- or host-type Treg cells in the mixed chimeric NOD mice. Mixed chimerism was induced by transplanting TCD-BM from either WT or PD-L1^{-/-} NOD mice together with TCD-BM from H-2^{b/g7} F1 donors. 60 days after HCT, percentage of donor-type (CD45.2⁺) or host-type (CD45.1⁺) Treg cells (TCRβ⁺Foxp3⁺CD4⁺) among donor- or host-type CD4⁺ T cells in the spleen, PanLN, and pancreas were measured. Representative patterns and Mean ± SEM of percentage of Tregs (Foxp3⁺) among (A) host-type or (B) donor-type CD4⁺ T cells in spleen, pancreatic LN, and pancreas are shown. N=6-9.

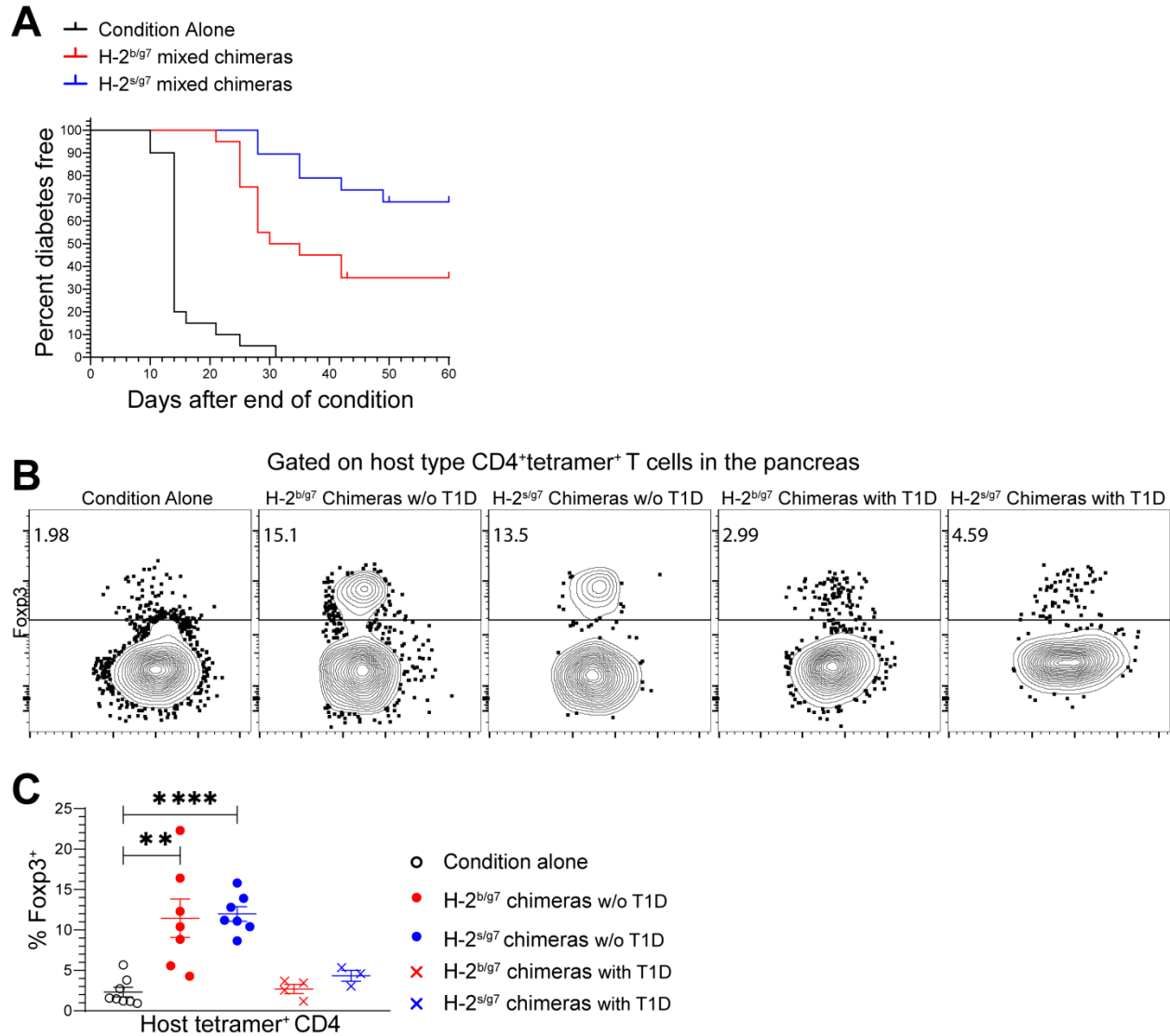


Fig S19: Expansion of antigen-specific pTreg cells in the pancreas is critical for preventing T1D in Haplo-MC BDC2.5 NOD mice. Haplo-MC in BDC2.5 NOD mice were established with BM cells from H-2^{b/g7} or H-2^{s/g7} donors as described in Fig. S3. The Haplo-MC mice and control mice given conditioning alone were monitored for T1D development by checking blood glucose. The T1D development curve is shown in (A). 60 days after HCT, the mixed chimeras with or without hyperglycemia was measured for percentage of Foxp3⁺ Treg cells among host-type I-A^{g7}-HIP-2.5-tetramer⁺ autoreactive CD4⁺ T cells. (B) Representative patterns of Tetramer⁺FoxP3⁺CD4⁺ T cells. (C) Mean ± SEM of percentage of Foxp3⁺ Treg cells among I-A^{g7}-HIP-2.5- tetramer⁺ autoreactive CD4⁺ T cells. There were 4-8 mice in each group. **p<0.01, ****p<0.0001.

Supplemental methods

Induction of mixed chimerism with ATG + CY+PT+ condition regimen

Recipient mice were given daily I.P. injection of cyclophosphamide (Cy, Sigma-Aldrich), 50mg/kg for WT NOD and adult-thymectomized female NOD mice, 40mg/kg for BDC 2.5 NOD, from D -12 to D-1; Pentostatin (PT, Sigma-Aldrich) 1mg/kg on D-12, D-9, D-6, D-3; and anti-thymocyte globulin (ATG, Accurate Chemical & Scientific Corporation) 25mg/kg, on D-12, D-9, D-6. On the day of HCT (D0), Recipients were injected intravenously with BM and SPL cells from donor mice mixed with 500ug purified depleting anti-mouse CD4 mAb (clone GK1.5, purchased from BioXcell). 6 weeks later, peripheral blood was collected from mice received HCT after conditioning or control mice received conditioning only and analyzed by flowcytometry.

Histopathology staining and insulinitis evaluation

Pancreas was fixed in 10% formalin solution and embedded in paraffin blocks. 2 slides were made for each level, and 3 different levels were sectioned for each sample. The distance between each level was 75 microns, and a total of 6 slides from each sample were cut and stained with H&E. The number of islets with insulinitis, peri-insulinitis or insulinitis-free in all 6 slides were counted, and then the percentage of each severity level among all islets from this mouse were calculated.

In vivo Treg depletion.

A mouse model to allow donor or host specific Treg depletion was set up as illustrated in Fig 9A, using mice (see table S1) in which diphtheria toxin (DT, purchased from Sigma-Aldrich) can be used to specifically ablate FoxP3⁺ T cells. 45-60 days after HCT, 40ug/kg DT was injected to mixed chimeric mice intraperitoneally every 3 days for 21 days. The last two injections on day 16 and 19 were reduced to 20ug/kg if body weight decreased by more than 20%.

Induction of host lymphocyte PD-L1^{-/-} mixed chimerism and induction of mixed chimerism under TBI conditioning with WT NOD.

Recipients were given 950 cGy total body irradiation (TBI). A cell suspension consisting of T cell depleted (TCD) BM from (B6xg7) F1 mice (7.5×10^6) or (SJLxg7) F1 mice (7.5×10^6) and TCD BM from WT NOD or PD-L1^{-/-} NOD mice (5×10^6) was injected through the tail vein 8-10 hours after irradiation.

Isolation of lymphocytes from pancreas

Pancreas was kept in FACs buffer (PBS containing 2mM EDTA and 2% BSA) on ice after harvest. It was minced quickly with a small curved scissors and mashed through a 70um strainer. Cell suspension was centrifuged and re-suspended in 6ml of 35% Percoll (Sigma-Aldrich , Cat# P1644-1L) solution for each pancreas, carefully laid above 3ml of 70% Percoll solution, centrifuged at 1200g at room temperature for 25min. After centrifuging, cells were collected from the middle layer, washed with FACs buffer, and then stained with surface antibody or tetramer antibody for flowcytometry analysis.

Release dendritic cells from spleen.

Spleen was harvested and kept in cold PBS. 5ml digestion buffer [RPMI containing 10% fetal bovine serum, collagenase D (0.15U/ml), and DNase I (0.2mg/ml)] was carefully injected into each spleen. Specimens were placed on an orbital shaker (80 rpm) and incubated at 37°C for 50 min. After digestion, tissue was mashed through a 70 µm cell strainer and washed with FACs buffer.

Flowcytometry staining

Surface markers were stained at 4°C for 15-20 min following the incubation with CD16/32 (BioXcell, Cat#. BE0307) and aqua viability dye (Invitrogen, Cat#. L34957). All intracellular

staining including FoxP3, Helios and CTLA-4 were performed with the Foxp3 / Transcription Factor Staining Buffer Set (eBioscience, Cat#. 00-5523-00) after surface staining. Detailed antibody information is listed in table S2. Flowcytometry analyses were performed with a CyAn ADP Analyzer (Beckman Coulter) or LSRFortessa (BD Bioscience).

Tetramer staining.

APC-labeled HIP 2.5 tetramer (I-A^{g7} LQTLALWSRMD), APC- labeled control tetramer (I-A^{g7} PVSKMRMATPLLMQA), PE-labeled NRP-V7 tetramer (H-2K(d) KYNKANVFL), PE- labeled control tetramer (H-2K(d) KYQAVTTTL) were obtained from the National Institutes of Health Tetramer Facility (Atlanta, GA). Cells were first blocked with CD16/32 for 60min at 37°C, and then incubated with labeled tetramers for 90 min at 37°C, both CD16/32 and tetramers were diluted with complete culture media. Cells were then washed with FACs buffer and continued to regular surface marker and intracellular staining.

Table S1: Animals

Mouse	Source	Cited as
NOD/ShiLtJ	Jackson Laboratory, stock No:001976	WT NOD
NOD.Cg-Tg(TcraBDC2.5,TcrbBDC2.5)1Doi/DoiJ	Jackson Laboratory, stock No:004460	BDC2.5 NOD
NOD/ShiLtJ-Tg(Foxp3-HBEGF/EGFP)1Doi/J	Jackson Laboratory, stock No:028763	FoxP3 ^{DTR} NOD
B6.NOD-(D17Mit21-D17Mit10)/LtJ	Jackson Laboratory, stock No: 003300	PD-L1 ^{-/-} NOD
NOD.B6-Cd274tm1Shr/J	Jackson Laboratory, stock No: 018307	g7
SJL/J	Jackson Laboratory, stock No: 000686	SJL
C57BL/6	National Cancer Institute	B6
B6.129(Cg)-Foxp3tm3(DTR/GFP)Ayr/J	Jackson Laboratory, stock No: 016958	FoxP3 ^{DTR} B6
(B6xg7)F1	backcrossing B6♀ to g7♂	(B6xg7)F1 or H-2 ^{b/g7} F1
(SJLxg7)F1	backcrossing SJL♀ to g7♂	(SJLxg7)F1 or H-2 ^{s/g7} F1
FoxP3 ^{DTR} F1	backcrossing FoxP3 ^{DTR} B6♀ to g7♂	FoxP3 ^{DTR} F1

Table S2: Antibodies

Antigen	Clone	Conjugation	Manufacturer	Cat#
B220	RA3-6B2	APC-eFlour780	ebioscience	47-0452-82
CD45.1	A20	APC-eFlour780	ebioscience	47-0453-82
CD45.2	104	APC-eFlour780	ebioscience	47-0454-82
CD62L	MEL-14	APC-eFlour780	ebioscience	47-0621-82
CD4	RM4-5	APC/Fire750	Biolegend	109246
TCR	H57-597	APC/Fire750	Biolegend	100568
CD45.1	A20	APC	ebioscience	17-0453-82
CD45.2	104	APC	ebioscience	17-0454-82
FoxP3	FJK-16s	APC	ebioscience	17-5773-82
Helios	22F6	APC	ebioscience	17-9883-42
CD317 (PDCA-1)	eBio927	APC	ebioscience	17-3172-82
TCR β	H57-597	APC	ebioscience	17-5961-83
CD304 (Neuropilin-1)	3DS304M	APC	ebioscience	17-3041-82
B220	RA3-6B2	biotin	eBioscience	13-0452-82
CD11b	M1/70	biotin	ebioscience	13-0112-82
CD11c	N418	biotin	ebioscience	13-0114-81
F4/80	BM8	biotin	ebioscience	13-4801-82
Ly-6G/Ly-6C	RB6-8C5	biotin	ebioscience	13-5931-82
CD45.1	A20	biotin	ebioscience	13-0453-82
CD45.2	104	biotin	ebioscience	13-0454-82
CD11b	M1/70	BUV395	BD	563553
CD8	53-6.7	BUV395	BD	563786
CD44	IM7	BUV395	BD	740215
TCR β	H57-597	BUV395	BD	742485
B220	RA3-6B2	BV421	BD	562922
FR4	12A5	BV421	BD	744119
CD8	53-6.7	BV605	BD	563152
CD357 (GITR)	DTA-1	BV605	BD	740428
TCR β	H57-597	BV605	Biolegend	109241
CD4	H129.19	BV711	BD	740684
CD8	53-6.7	BV711	BD	563046
CD278 (ICOS)	7E.17G9	BV711	BD	740763
TCR V β 4	KT4	BV711	BD	743023
CD279 (PD1)	29F.1A12	BV711	Biolegend	135231
CD11c	N418	BV711	Biolegend	117349
TCR β	H57-597	BV711	Biolegend	109243

CD45.1	A20	eFluor 450	ebioscience	48-0453-82
CD45.2	104	eFluor 450	ebioscience	48-0454-82
B220	RA3-6B2	eFluor 450	ebioscience	48-0452-82
CD11b	M1/70	eFluor 450	ebioscience	48-0112-82
FoxP3	FJK-16s	eFluor 450	ebioscience	48-5773-82
Helios	22F6	eFluor 450	ebioscience	48-9883-42
B220	RA3-6B2	FITC	BD	553088
CD11c	N418	FITC	ebioscience	11-0114-85
CD4	GK 1.5	FITC	ebioscience	11-0041-82
CD45.1	A20	FITC	BD	553775
CD45.2	104	FITC	BD	553772
FR4	eBio12A5	FITC	ebioscience	11-5445-80
H2Kd	SF1-1.1	FITC	BD	553565
IA/IE	M5/114.15.2	FITC	ebioscience	11-5321-82
TCR V β 4	KT4	FITC	BD	553365
FoxP3	MF23	Alexa Fluor 488	BD	560403
CD44	IM7	FITC	BD	553133
TCR β	H57-597	FITC	ebioscience	11-5961-85
CD19	eBio1D3	PE-cy7	ebioscience	25-0193-82
CD3	145-2C11	PE-cy7	ebioscience	25-0031-82
CD45.1	A20	PE-cy7	ebioscience	25-0453-82
CD45.2	104	PE-cy7	ebioscience	25-0454-82
CD73	eBioTY/11.8 (TY/11.8)	PE-cy7	ebioscience	25-0731-82
CD8	53-6.7	PE-cy7	ebioscience	25-0081-82
IgM	II/41	PE-cy7	ebioscience	25-5790-82
IgD	11-26c	PE-cy7	ebioscience	25-5993-82
CD127 (IL-7Ra)	eBioSB/199 (SB/199)	PE-cy7	ebioscience	25-1273-82
CD317 (PDCA-1)	eBio927	PE-cy7	ebioscience	25-3172-82
CD172a	P84	PE	ebioscience	12-1721-82
CD44	IM7	PE	ebioscience	12-0441-83
CD8	53-6.7	PE	ebioscience	12-0081-82
CD152 (CTLA-4)	UC10-4B9	PE	ebioscience	12-1522-82
Ly-6G and Ly-6C	RB6-8C5	PE	BD	553128
CD11b	M1/70	PE	ebioscience	12-0112-83
CD274 (PD-L1)	MIH5	PE	ebioscience	12-5982-82
TCR Va2	B20.1	PE	BD	553289
foxP3	NRRF-30	PE	ebioscience	12-4771-82
CD45.2	104	PerCP-Cy5.5	ebioscience	45-0454-82
CD11b	M1/70	PerCP-Cy5.5	ebioscience	101228
CD73	eBioTY/11.8 (TY/11.8)	PerCP-eFluor 710	ebioscience	46-0731-82

CD304 (Neuropilin-1)	3DS304M	PerCP-eFluor 710	ebioscience	46-3041-82
CD4	RM4-5	Qdot605	Invitrogen	q10092
Streptavidin	N/A	Alexa Fluor 350	Molecular Probes	S11249
Streptavidin	N/A	APC	ebioscience	17-4317-82
Streptavidin	N/A	APC-eFlour780	ebioscience	47-4317-82
Streptavidin	N/A	PE-cy7	ebioscience	25-4317-82
Armenian Hamster IgG isotype	eBio299Arm	PE	ebioscience	12-4888-81
Rat IgG2a, κ isotype	ebr2a	PE	ebioscience	12-4321-82
Rat IgG2b, κ isotype	R35-38	BV605	BD	563145
Rat IgG2b, κ isotype	R35-38	BV711	BD	563045